Biochimica et Biophysica Acta 818 (1985) 235–250
Elsevier

BBA 72709

Kinetics of ($Na^+ + K^+$)-ATPase: analysis of the influence of Na^+ and K^+ by steady-state kinetics

Igor W. Plesner [a] and Liselotte Plesner [b]

[a] *Department of Chemistry, Physical Chemistry Division, and* [b] *Institute of Biophysics, University of Aarhus, DK-8000 Aarhus C (Denmark)*

(Received April 18th, 1985)

Key words: ($Na^+ + K^+$)-ATPase; Steady-state kinetics; Cation binding; Multicycle kinetic model; Biphasic substrate kinetics; (Bovine brain)

The influence of Na^+ and K^+ on the steady-state kinetics at 37°C of ($Na^+ + K^+$)-ATPase was investigated. From an analysis of the dependence of slopes and intercepts (from double-reciprocal plots or from Hanes plots) of the primary data on Na^+ and K^+ concentrations a detailed model for the interaction of the cations with the individual steps in the mechanism may be inferred and a set of intrinsic (i.e. cation independent) rate constants and cation dissociation constants are obtained. A comparison of the rate constants with those obtained from an analogous analysis of Na^+-ATPase kinetics (preceding paper) provides evidence that the ATP hydrolysis proceeds through a series of intermediates, all of which are kinetically different from those responsible for the Na^+-ATPase activity. The complete model for the enzyme thus involves two distinct, but doubly connected, hydrolysis cycles. The model derived for ($Na^+ + K^+$)-ATPase has the following properties: (1) The empty, substrate free, enzyme form is the K^+-bound form E_2K. Na^+ ($K_d = 9$ mM) and MgATP ($K_d = 0.48$ mM), in that order, must be bound to it in order to effect K^+ release. Thus Na^+ and K^+ are simultaneously present on the enzyme in part of the reaction cycle. (2) Each enzyme unit has three equivalent and independent Na^+ sites. (3) K^+ binding to high-affinity sites ($K_d = 1.4$ mM) on the presumed phosphorylated intermediate is preceded by release of Na^+ from low-affinity sites ($K_d = 430$ mM). (4) The stoichiometry is variable, and may be Na : K : ATP = 3 : 2 : 1. To the extent that the transport properties of the enzyme are reflected in the kinetic ATPase model, these properties are in accord with one of the models shown by Sachs ((1980) J. Physiol. 302, 219–240) to give a quantitative fit of transport data for red blood cells.

Introduction

The purpose of the present article is to analyze in detail the influence of Na^+ and K^+ on kinetic results obtained with ($Na^+ + K^+$)-ATPase, i.e. the activity measured at millimolar substrate and $K^+ + Na^+$, and to develop a model capable of quantitatively explaining the data in a manner analogous to those of the Na^+-enzyme [1] (preceding paper). Such a model, detailing the actions of the monovalent cations, is a prerequisite for providing an answer to the question: to what extent are the kinetic intermediates present in Na^+-ATPase activity a part of the main hydrolysis cycle at high (millimolar) substrate concentration and in the presence of both Na^+ and K^+. Also, to the extent that a kinetic model inferred from steady-state data in vitro accurately reflects the properties of the transport system in vivo, and that the kinetic states in the hydrolysis cycle represent the states associated with the concomitant cation transport, Na^+-K^+ exchange in this case, across

the membrane, one may hope by this means to contribute to elucidating the question of the type of transport, simultaneous or consecutive, involved in the normal action of the sodium pump.

We have previously demonstrated [2] that the steady-state kinetics of $(Na^+ + K^+)$-ATPase and of Na^+-ATPase (micromolar substrate) are well represented by minimal models (almost) identical in form, which when the concentration of Mg^{2+} is sufficiently high (> 5 mM), consist of no more than three kinetically distinguishable intermediates, each of which in turn may represent pools of cation-liganded intermediates in internal equilibrium. This property of the model simplifies the expressions for the kinetic parameters in terms of effective rate constants considerably.

The procedure is the same as the one used in connection with the Na^+-ATPase. We study separately the form (i.e. the cation dependence) of the slope and intercept of double-reciprocal plots of the primary steady-state rate data. This permits a study of the interference of the ligands with separate parts of the reaction cycle [1]. In the present case the data seem less complicated than for the Na^+-ATPase in that also the intercept ($V^{-1}_{max,app}$) may be resolved, so that when combined with the slope analysis a complete minimal model for the entire reaction cycle, as well as estimates of rate constants and binding constants, can be obtained based on the steady-state data.

After a brief presentation of the experimental results, in the following section Data analysis and Discussion we first perform a preliminary analysis of the slope data. From qualitative considerations it is shown that all but two of the simple possible models can be excluded from further consideration, and that one of the two possibilities remaining appears to be in conflict with other kinetic data reported recently [3].

Using the expressions for slope and intercept (of double-reciprocal plots) for the most likely model inferred from this, the data are analyzed in detail. It is found that 2 K^+ ions and 3 Na^+ ions interact with the enzyme in such a way that Na^+ and ATP, in that order, must be bound to the potassium-bound enzyme (probably the occluded K^+-form) in order to release K^+ prior to the splitting of ATP, and thus Na^+ and K^+ are simultaneously bound to the enzyme in part of the hydrolysis cycle. Furthermore, the analysis reveals that the intrinsic, i.e. cation-independent rate constant characterizing the ATP-splitting step in the mechanism seems to be about 30-times as large as the corresponding rate constant found for Na^+-ATPase [1]. When combined with other recent evidence [4] these results quantitatively support the notion proposed earlier [5,6] that the hydrolysis cycles of the two activities are distinct, but must be combined in order to represent the action of a single enzyme in the entire substrate range. Such a model provides a mechanism of 'memory': at any time an enzyme molecule 'remembers' which cycle it is presently engaged in, because its state uniquely associates it with a particular cycle in the mechanism.

A preliminary account of some of the results in this paper was presented at the Fourth International Conference on Na,K-ATPase, Cambridge (U.K.), Aug. 5–11, 1984.

Materials and Methods

Enzyme preparation, procedures, and materials have been detailed, (see Ref. 1, preceding paper). For the present investigation the following changes are relevant.

Assay of ATP hydrolysis rate. The enzyme preparation containing 2 mg protein per ml was diluted 5–150-times for the kinetic experiments. A further dilution of 10-times took place in the assay. Incubation time was 5–30 min and temperature of the assay 37°C. Substrate concentration was between 0.15 and 5 mM MgATP at constant $Mg^{2+}_{free} = 7$ mM. In each specific run the substrate concentration was varied by a factor of about 10. However, the substrate range was different in different experiments as demanded by the combination of Na^+ and K^+ in the individual run. P_i was determined according to the method of Ottolenghi [7], or ATP hydrolysis was measured by the method of Lindberg and Ernster [8] with a specific activity of the substrate of 1400– 41 000 cpm · nmol^{-1}.

All kinetic results were standardized so as to correspond to the undiluted enzyme with a concentration $E_0 = 0.66$ μM.

Experimental results

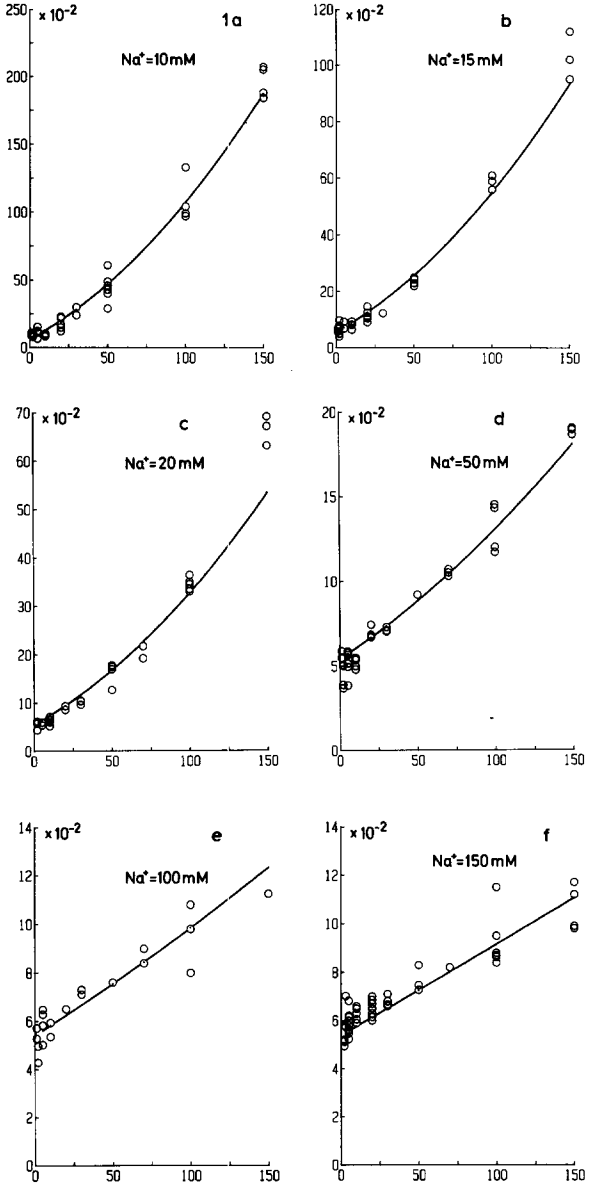

Fig. 1. The slope from double-reciprocal plots ($1/v$ vs. $MgATP^{-1}$) as a function of $[K^+]$ at the Na^+ concentrations indicated. The curves were calculated using Eqn. 2 and the kinetic parameters in Table II. The assay conditions are described in Materials and Methods. The buffer was histidine, 30 mM, pH 7.4 at 37°C and the free Mg^{2+} concentration was 7 mM throughout. All rate measurements were normalized to correspond to undiluted enzyme (2 mg of protein/ml.) Ordinate; slope in min; abscissa: $[K^+]$ in mM.

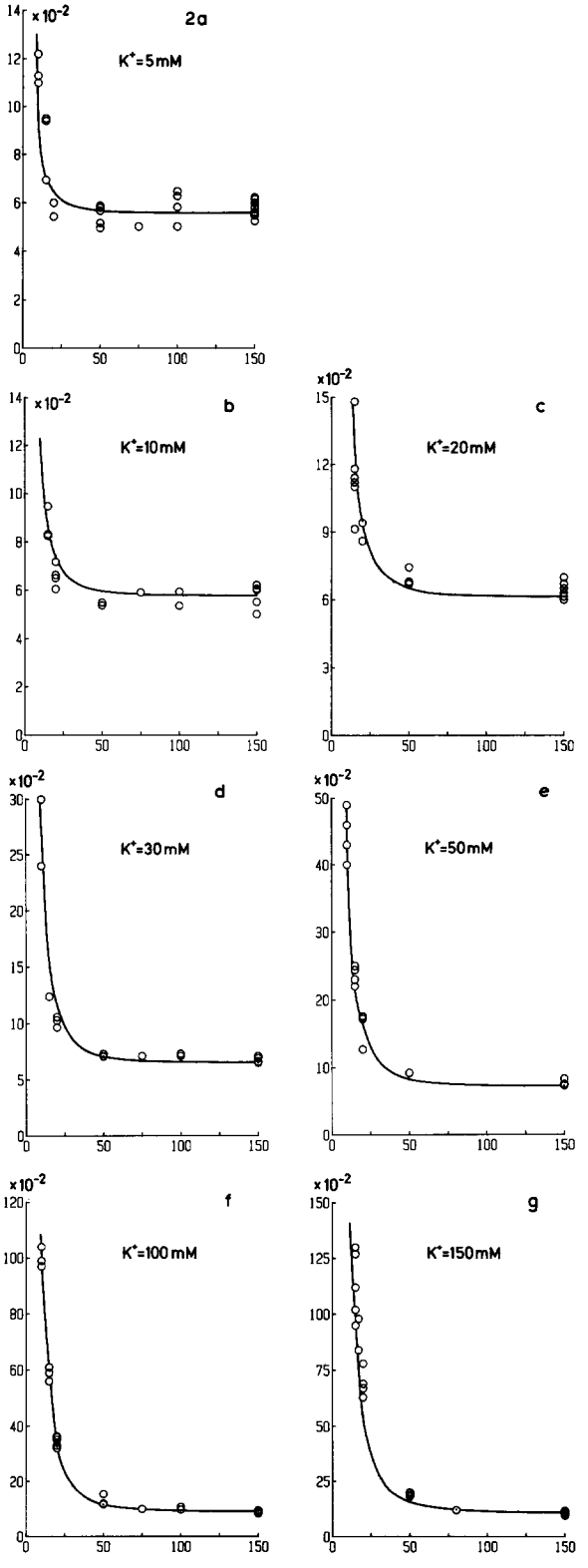

Fig. 2. The variation of the slope from double-reciprocal plots ($1/v$ vs. $1/MgATP$) with $[Na^+]$ at the K^+ concentrations indicated. The curves were calculated using Eqn. 2 and the kinetic parameters in Table II. Ordinate: slope in min; abscissa: $[Na^+]$ in mM.

The slope from primary double-reciprocal plots, as a function of $[K^+]$ at various Na^+ concentrations is shown in Fig. 1, and in Fig. 2 the slope data are plotted as a function of $[Na^+]$. It is seen that while Na^+ shows strong activation at small concentrations and saturation of this effect at higher concentrations, K^+ exhibits inhibition which becomes approximately linear at high Na^+ concentration. The Na^+ effect resembles that seen for Na^+-ATPase [1] except that Na^+ seems to be essential, i.e. there is no approach to a finite limit as $[Na^+] \rightarrow 0$ (except, of course, that for $[Na^+] = 0$ we would measure the K^+-inhibited '0-ATPase'). Note, however, that the slopes found with $(Na^+ + K^+)$-ATPase are in most cases 20–30-times higher than the values found for Na^+-ATPase.

At low and intermediate Na^+ concentrations, K^+ inhibits strongly, and the form of the curves indicates that more than one, probably two, potassium ions are involved. The inhibition is in part overcome by higher concentrations of Na^+, and at 150 mM Na^+ the inhibition appears linear, with a very low sensitivity, i.e. a high apparent slope inhibition constant for K^+.

At high $[Na^+]$ a decrease in $[K^+]$ leads to a very pronounced decrease in the slope (Fig. 3), which approaches values characteristic of the Na^+-enzyme.

The intercept data are shown in Fig. 4. It is noted that irrespective of the Na^+ concentration

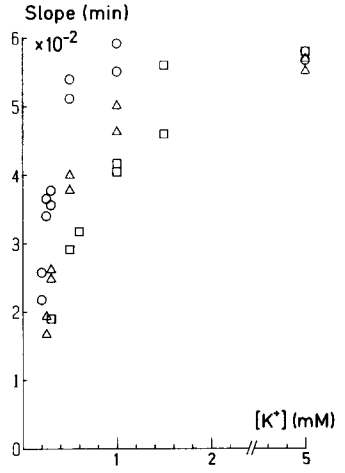

Fig. 3. The slope from double-reciprocal plots ($1/v$ vs. $MgATP^{-1}$) as a function of $[K^+]$ at low K^+ concentrations. The Na^+ concentrations were 50 mM (○), 100 mM (△), and 150 mM (□).

K^+ shows strong (high-affinity) activation at low (< 3 mM) K^+ concentrations, while low-affinity K^+ inhibition is observed for concentrations higher than 20 mM. In contrast, Na^+ is inhibitory at low K^+ concentrations, but this inhibition is abolished completely as the K^+ concentration is increased. The latter property proves to be an important diagnostic because, as shown in the Data analysis and Discussion (next section), it enables us to

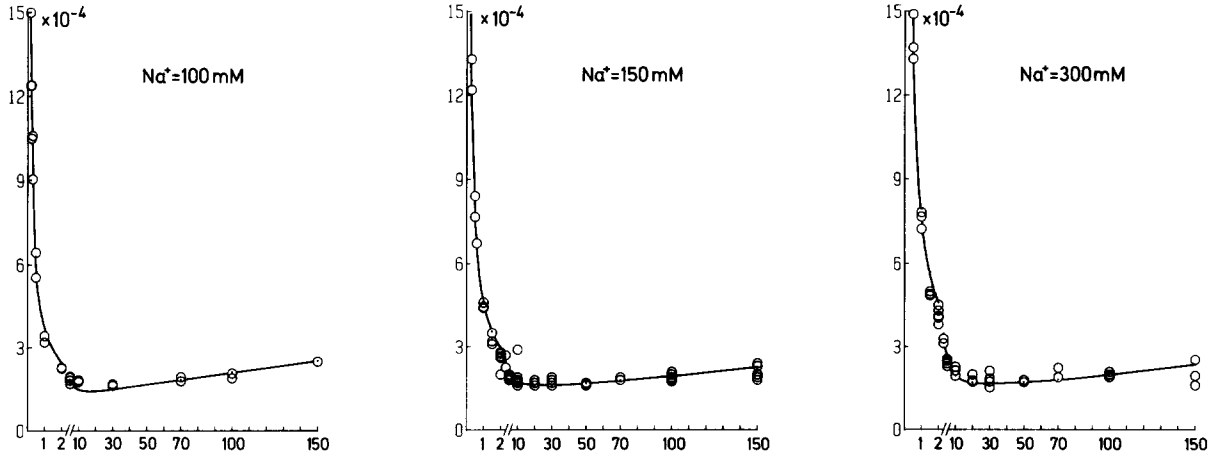

Fig. 4. The ordinate intercept $V^{-1}_{m,app}$ from primary double-reciprocal plots ($1/v$ vs. $1/MgATP$) plotted against the K^+ concentration at the Na^+ concentrations indicated. The curves were calculated using Eqn. 10 and the kinetic parameters in Table II. Ordinate: intercept in $nmol^{-1} \cdot ml \cdot min$; abscissa: $[K^+]$ in mM.

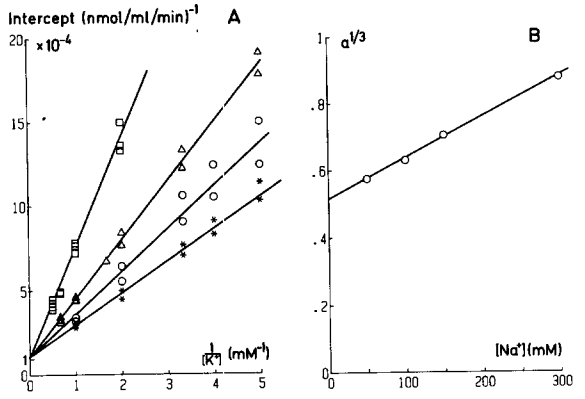

Fig. 5. (A) The ordinate intercept $V_{m,app}^{-1}$ from primary double reciprocal plots ($1/v$ vs. 1/MgATP) plotted against the reciprocal K^+-concentration at various Na^+ concentrations. The range of [K^+] was 0.2–2 mM. The Na^+ concentrations were 50 mM (*), 100 mM (○), 150 mM (△), and 300 mM (□). The lines are the least-squares regression lines. (B) The cubic roots of the calculated slopes of the lines in Fig. 5(A) plotted against the Na^+ concentration. The line is the least-squares regression line.

distinguish between two possibilities for the order in which Na^+ is released from and K^+ binds to the (phosphorylated) enzyme in the course of the hydrolysis of substrate. Fig. 5A is a plot of the intercept against the reciprocal K^+ concentrations, showing a linear relationship, used for parameter estimation, see next section. From Figs. 1–5 it is apparent, then, that only at small concentrations, less than 3 mM, does K^+ activate, and then only

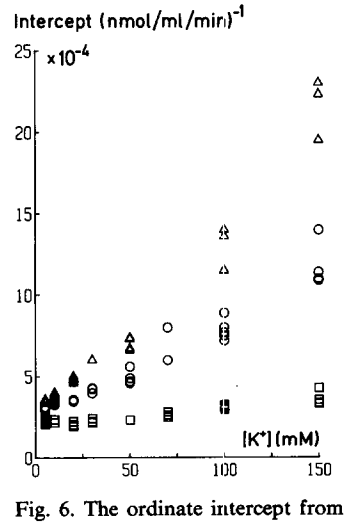

Fig. 6. The ordinate intercept from primary double-reciprocal plots ($1/v$ vs. 1/MgATP) plotted against the K^+ concentration at [Na^+] 50 mM (□), 20 mM (○), and 15 mM (△).

the apparent V_{max}. In all other cases K^+ inhibits the ($Na^+ + K^+$)-ATPase. For Na^+-ATPase (see previous article) we found that K^+ was inhibitory at all concentrations, for slope as well as V_{max} data. At low [Na^+], an increase in the K^+ concentration leads to a very pronounced increase in the ordinate intercept (Fig. 6), which approaches values characteristic of the Na^+-enzyme.

Data analysis and Discussion

A detailed analysis of the data and the determination of intrinsic rate parameters and binding constants requires a precise model. In order to infer the type of model (for the interaction of Na^+ and K^+), we first consider the slope data in Fig. 1. The observed inhibition by K^+ indicates that K^+ must leave the enzyme prior to the splitting of ATP, and the qualitative behavior of the slope in Fig. 1 indicates the involvement of two potassium ions. If so, the slope as a function of [K^+] must be of the form

$$\text{slope} = a + b\cdot[K^+] + c\cdot[K^+]^2 \qquad (1)$$

where a, b, and c are functions of Na^+. A preliminary fit is obtained by fitting Eqn. 1 to the data in Fig. 1. Using a linear regression routine, the results for a, b, and c as a function of Na^+ are shown in Table I. (Note that the theoretical curves in Figs. 1 and 2 are not obtained by using these results. They have been calculated using the equa-

TABLE I

VALUES OF THE COEFFICIENTS a, b AND c IN THE PRELIMINARY FIT OF THE SLOPE DATA TO

$$\text{slope} = a + b\cdot[K^+] + c\cdot[K^+]^2$$

OBTAINED BY REGRESSION ANALYSIS OF THE DATA IN Fig. 1 AT VARIOUS Na^+ CONCENTRATIONS ([K^+] IN mM)

Na^+ (mM)	$a(\times 10^2)$	$b(\times 10^4)$	$c(\times 10^5)$
10	5.2	68	4.0
15	6.6	14	3.7
20	5.6	9.2	2.0
50	5.0	6.7	0.19
100	5.2	6.1	−0.1 [a]
150	5.6	5.7	−0.17 [a]

[a] Not significantly different from zero.

tion given below after a determination of the various parameters as described in the following). It is clear from Table I that, with reference to Eqn. 1, the coefficient a is practically constant, b decreases to a finite limit, and c decreases to zero, as $[Na^+]$ is increased. From a consideration of the various possibilities (see Appendix A) it is seen that only models (vii) and (viii) satisfy these requirements in a qualitative way. Of these, model (viii) requires that ATP binds directly to the enzyme-potassium adduct. However, from experiments on the kinetic influence of K^+ in the absence of Na^+ reported recently [3] it appears that even in the presence of millimolar ATP concentrations, K^+ was a competitive inhibitor, indicating that K^+ and nucleotide are mutually exclusive (see below for further discussion of this point). On this basis the model of choice is of the type listed in Appendix A as model (vii). An explicit version of this model, with three binding sites assumed for

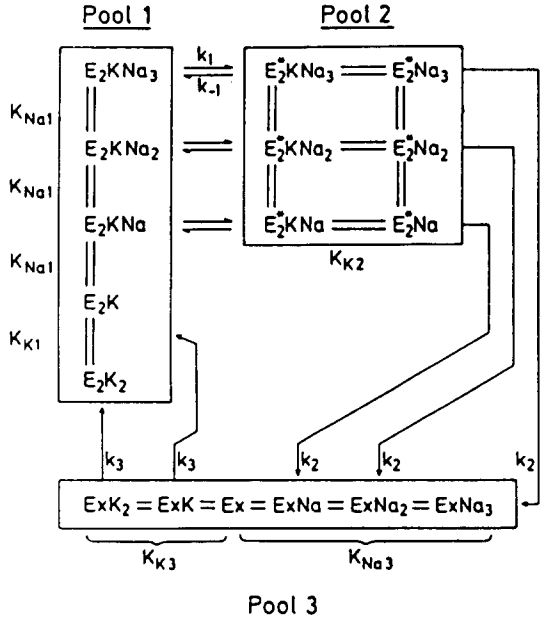

Fig. 7. The proposed minimal model describing the interaction of Na^+ and K^+ with the $(Na^+ + K^+)$-ATPase. The presence of substrate MgATP on the enzyme is indicated by an asterisk. Within the boxes drawn around the species in a pool, rapid internal equilibrium is indicated with double lines, and the dissociation constants are indicated along appropriate equilibria. The dissociation constant for Na^+ in pool 2 is equal to that in pool 1. The rate constants indicated are the intrinsic values.

Na^+, is shown in Fig. 7. The simultaneous presence of Na^+ and K^+ on the enzyme is in line with results by Yamaguchi and Tonomura [9].

For such a model, with an arbitrary number, n, of binding sites for Na^+, the slope function is found using Cha's method [10] for expressing apparent rate constants in partial equilibrium models. The result is, using the dissociation constants indicated in Fig. 7:

$$\text{slope} = \frac{1}{k_1 E_0}\left[\frac{(1+\text{Na}/K_{\text{Na1}})^n}{(1+\text{Na}/K_{\text{Na1}})^n - 1} + \frac{\text{K}/K_{\text{K1}}}{(1+\text{Na}/K_{\text{Na1}})^n - 1}\right] \times [1+\text{K}/K_{\text{i slope}}] \quad (2)$$

where

$$K_{\text{i slope}} \equiv \frac{k_2 K_{\text{K2}}}{k_{-1}} \quad (3)$$

is an effective slope inhibition constant for K^+ – the only one detectable at high Na^+ concentration, because the first bracketed term in Eqn. 2 becomes equal to 1 when $[Na^+] \gg K_{\text{Na1}}$, and hence

$$\text{slope} = \frac{1}{k_1 E_0}(1+\text{K}/K_{\text{i slope}}) \quad (4)$$

This behaviour is in accord with the data in Fig. 1 for $Na^+ = 150$ mM. From this line $k_1 E_0$ and $K_{\text{i slope}}$ may be determined (Table II).

The model in Fig. 7 also predicts that the quantity Q defined by

$$Q \equiv \frac{\text{slope} \cdot k_1 E_0}{1+\text{K}/K_{\text{i slope}}} \simeq 1 + \frac{\text{K}}{K_{\text{K1}}(1+\text{Na}/K_{\text{Na1}})^n} \quad (5)$$

is a linear function of $[K^+]$ intercepting the ordinate axis at 1 (when $[Na^+] > K_{\text{Na1}}$), the slope, α, of which decreases as $[Na^+]$ is increased. This is verified by Fig. 8. The number, n, of Na^+-binding sites involved may then be found, since from Eqn. 5 we have

$$\alpha^{-1/n} = (K_{\text{K1}})^{1/n}\left(1 + \frac{\text{Na}}{K_{\text{Na1}}}\right) \quad (6)$$

A plot corresponding to Eqn. 6, for $n = 2$ and $n = 3$, where α was determined by linear regression from the data in Fig. 8A, is shown in Fig. 8B, from which we deduce that $n = 3$. The correspond-

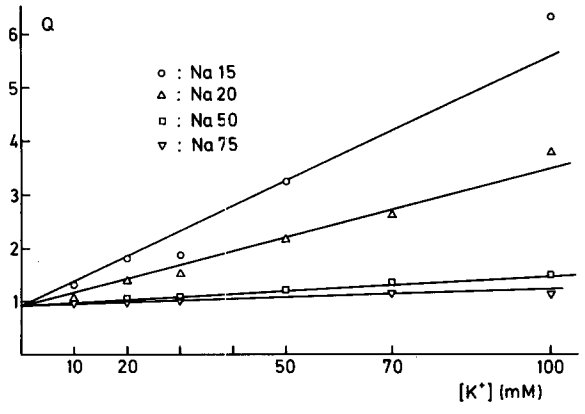

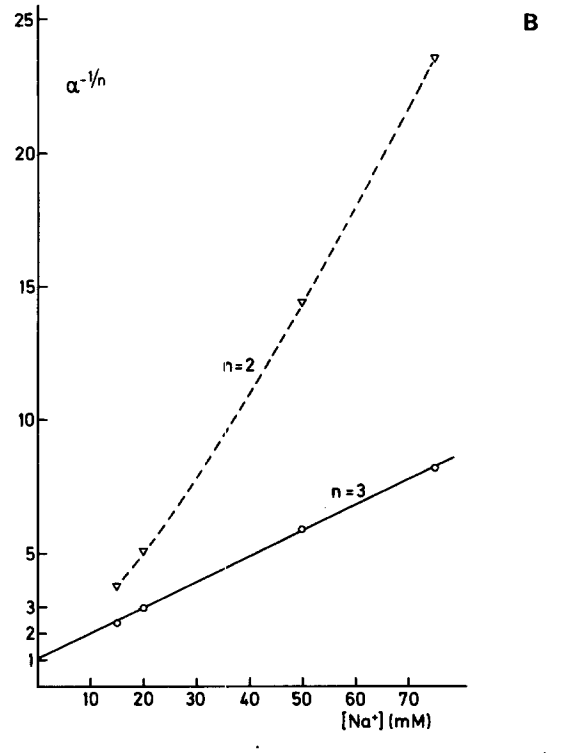

Fig. 8. (A) The quantity Q (see text) as a function of $[K^+]$ at various intermediate concentrations of Na^+ as indicated. A straight line relationship, with an intercept of 1 is predicted by the model in Fig. 7. Q was calculated using mean values of the slope data shown in Figs. 1 and 2. (B) The reciprocal of the square root ($n = 2$) and the cubic root ($n = 3$) of α, the slope lines from Fig. 8(A), as a function of $[Na^+]$.

ing line in Fig. 8B was used to estimate K_{K1} and K_{Na1}.

In order to complete the estimation of the kinetic parameters in Fig. 7 we turn next to the data for

TABLE II

VALUES OF CATION INDEPENDENT KINETIC PARAMETERS OBTAINED FOR THE MODEL IN Fig. 7.

Dissociation constants for				Rate constants	
Na^+	(mM)	K^+	(mM)		
K_{Na1}	9	$K_{i\,slope}$	150	$k_1(M^{-1}\cdot s^{-1})$	$4.7\cdot10^5$
$K_{Na2} = K_{Na1}$	9	K_{K1}	1.1	$k_{-1}(s^{-1})$	$2.2\cdot10^2$
K_{Na3}	429	K_{K2}	32	$k_2(s^{-1})$	$1\cdot10^3$
		K_{K3}	1.4	$k_3(s^{-1})$	$2.6\cdot10^2$

the intercept in Fig. 4. We have indicated in Fig. 7 only three kinetically distinguishable intermediates (equilibrium pools). It is well known that introducing more isomeric intermediates in a model does not change the overall form of the steady-state rate equation. For an interpretation of the present kinetic data for $(Na^+ + K^+)$-ATPase, in contrast to those for Na^+-ATPase, only one 'Ex-pool' (probably a phosphoenzyme pool) is sufficient.

For the 3-state model in fig. 7, the reciprocal apparent V_{max} is

$$V_{m,app}^{-1} = \frac{1}{E_0}\left(\frac{1}{k_2'} + \frac{1}{k_3'}\right) \tag{7}$$

where the primed k values are effective rate constants. k_2', the rate constant out of pool 2, is

$$k_2' = \frac{k_2}{1 + K/K_{K2}} \tag{8}$$

The form of the rate constant k_3' depends on the order in which Na^+ is released and K^+ is bound. There are two possibilities: either K^+ binds first to the Na^+-bound Ex which subsequently releases Na^+ (a simultaneous scheme), or Na^+ is released first, prior to K^+ binding (a consecutive scheme). For the intercept we obtain in the two cases (assuming only one K^+ binding site, see below):

$$\text{simultaneous: } V_{m,app}^{-1} = \frac{1}{E_0}\left\{\frac{(1+y_2)}{k_2} + \frac{(1+x_3)^3}{k_3} + \frac{x_3^3}{k_3 y_3}\right\} \tag{9}$$

$$\text{consecutive: } V_{m,app}^{-1} = \frac{1}{E_0}\left\{\frac{(1+y_2)}{k_2} + \frac{1}{k_3} + \frac{(1+x_3)^3}{k_3 y_3}\right\} \tag{10}$$

where we have used

$$x_3 \equiv \frac{[Na^+]}{K_{Na3}};\ y_2 \equiv \frac{[K^+]}{K_{K2}};\ y_3 \equiv \frac{[K^+]}{K_{K3}} \tag{11}$$

At constant (low) $[K^+]$, Eqns. 9 and 10 both show Na^+ inhibition. But at high K^+ concentrations, i.e. y_3 large, this is virtually abolished in the consecutive case, Eqn. 10, but not in the simultaneous case, Eqn. 9, because the middle term in brackets is independent of $[K^+]$. As already noted in the previous section, the data are in accord with the former prediction, but not with the latter. The consecutive model is therefore incorporated in Fig. 7.

At very low K^+ concentrations ($y_2 \approx 0$), Eqn. 10 predicts a linear dependence of $V_{m,app}^{-1}$ on $[K^+]^{-1}$:

$$V_{m,app}^{-1} \simeq \frac{1}{E_0}\left\{\frac{1}{k_2}+\frac{1}{k_3}+\frac{1}{k_3}\left(1+\frac{Na^+}{K_{Na3}}\right)^3 \cdot \frac{K_{K3}}{[K^+]}\right\}$$

$$\equiv b + a\cdot[K^+]^{-1} \tag{12}$$

A plot of the data for $[K^+] \leq 2$ mM is shown in Fig. 5A. We have then proceeded as follows:

(1) The slopes, a, determined by linear regression at various Na^+ concentrations using Eqn. 12 are used in a plot (Fig. 5B) of $a^{1/3}$ versus $[Na^+]$:

$$a^{1/3} = \left(\frac{K_{K3}}{k_3 E_0}\right)^{1/3}\left(1+\frac{[Na^+]}{K_{Na3}}\right) \tag{13}$$

from which we determine K_{K3}/k_3 and K_{Na3}.

(2) The entire sets of intercept data are used to estimate the parameters A and B in

$$V_{m,app}^{-1} = A + B\cdot[K^+] + a\cdot[K^+]^{-1} \tag{14}$$

using a linear regression routine. By comparing Eqns. 14 and 10, we have

$$A = \frac{1}{k_2 E_0} + \frac{1}{k_3 E_0} \tag{15}$$

$$B = (K_{K2}\cdot k_2 E_0)^{-1} \tag{16}$$

(3) From previous kinetic results [6], obtained at 20 mM K^+ and 150 mM Na^+, we have

$$k_2' = \frac{k_2}{1+[K^+]/K_{K2}} = 2.7\cdot 10^4\ \text{min}^{-1} \tag{17}$$

This allows the calculation of k_3 from the intercept value at the same ionic concentrations, since

$$V_{m,app}^{-1} = 1.7\cdot 10^{-4} = \frac{1}{k_2' E_0} + \frac{1}{k_3 E_0} + \frac{a(Na^+ = 150\ \text{mM})}{[K^+]} \tag{18}$$

Eqns. 15 and 16 then yield k_2 and K_{K2}, and, using Fig. 5B and Eqn. 13 we can calculate K_{K3}.

From the estimate, using the slope data above, of the 'effective' slope inhibition constant for K^+, $K_{i\ slope}$, Eqn. 3, we then have

$$k_{-1} = k_2 K_{K2}/K_{i\ slope} \tag{19}$$

which completes the determination of the kinetic parameters of the model in Fig. 7. The numerical values obtained by these procedures are collected in Table II and have been used for the calculation of the theoretical curves in the figures, using Eqns. 2 and 10, respectively.

In Fig. 7, two identical and equivalent sites for K^+ in pool 3 have been assumed. Also a non-liganded form of enzyme is absent in pool 1. It may be shown that the data and the analysis just described cannot distinguish whether one or two K^+ sites are present in the Ex pool, or whether an E_2 form is present in pool 1, if K^+ binds to E_2 with reasonably high affinity – a dissociation constant of the order 1 mM or less. But the E_2 form of the enzyme is known to have a high affinity for K^+ (or Rb^+) [11,12].

The model in Fig. 7 and Eqn. 10 provides a clear interpretation of the intercept data: At small K^+ concentrations, K^+ activates because it must be bound to the phosphoenzyme Ex prior to dephosphorylation. In this K^+ range, Na^+ inhibits because the Na^+-bound Ex-forms not able to bind K^+ are favored. Large K^+ concentrations overcome the Na^+ inhibition, but now the concentration of the nonreactive intermediates $E_2^*KNa_i$ is being increased at the expense of the reactive ones, E^*Na_i, and therefore (low affinity) inhibition is observed.

The model in Fig. 7 requires addition of Na^+ and ATP, in that order, before K^+ is released from the enzyme in the forward direction of ATP hydrolysis. As mentioned above, a model in which

ATP adds to the E_2K-form, with subsequent K^+ release and Na^+ binding, also yields a slope function in qualitative agreement with data. This latter possibility would be in line with evidence obtained by Glynn and Richards [13], by Glynn et al. [14], and by Forbush [15], who measured the increase in the rate of K^+ release from E_2K effected by ATP in the absence of added Na^+. Our conclusion on the basis of steady-state kinetic data that direct addition of ATP to E_2K prior to the addition of Na^+ seems less likely was based on (1) the observed K^+-nucleotide antagonism [3], (2) the fact that substrate inhibition of '0-ATPase' was not seen, even at high substrate concentration, which ought to occur if the inhibiting EK-adduct could also bind ATP, but not hydrolyze it due to the lack of Na^+, and (3) an estimate of the E-ATP dissociation constant when adopting this model, resulting in $K_{d,ATP} \approx 25$ mM. Our kinetic results, from measurements performed in histidine buffer, may not be directly comparable to those of Glynn et al. [13,14] which were carried out in Tris buffer, and Tris, in contrast to histidine, has a 'Na^+-effect' on the enzyme as determined by intrinsic as well as extrinsic (eosin maleimide) fluorescence [16]. It is of interest in this connection to report some recent kinetic results with the '0-ATPase' (data not shown): when the experiments were performed using Tris buffer in the presence of K^+, substrate inhibition was observed at larger ATP concentrations, in contrast to the situation with histidine where no such inhibition was observed.

The experiments of Glynn et al. [13,14] and Forbush [15] are supportive of the most widely used scheme for $(Na^+ + K^+)$-ATPase, the Albers-Post model, because in that model the activation (relative to the K^+-inhibited Na^+-ATPase reaction) of the enzyme with K^+ and high ATP concentrations depends on the acceleration by ATP of K^+ release from E_2K. It is a consequence of the Albers-Post scheme, however, that the intrinsic ATP splitting rate constant k_2 for $(Na^+ + K^+)$-ATPase should be smaller than or equal to the corresponding rate constant for Na^+-ATPase. This is not a requirement for the bicyclic model proposed earlier [5], according to which the hydrolysis cycles for Na^+-ATPase and $(Na^+ + K^+)$-ATPase are distinct. A more detailed argument has been reported recently [17]. Comparing the value of k_2 (Table II) found in the present work with the corresponding rate constant for Na^+-ATPase (see accompanying paper [1],) k_2 (Na^+-ATPase) ≈ 37 s^{-1}, it is seen that our kinetic results are not easily interpreted in terms of the Albers-Post scheme. This result, taken together with the recent analysis of Nørby et al. [4], indicating that the phosphorylated intermediates in the Na^+-ATPase cycle cannot be intermediates in the main hydrolysis cycle in $(Na^+ + K^+)$-ATPase activity, then favors the bicyclic model. When the results obtained here, in the accompanying paper [1], and in our recent report on '0-ATPase' [3] are combined, the model shown schematically in Fig. 9 is obtained.

The analysis outlined above was carried out in terms of slopes and intercepts, 'belonging' to the ATP hydrolysis in the Na^+,K^+-cycle. Likewise, in the preceding paper, the slope function 'belonging' to the hydrolysis in the Na^+-cycle was analyzed. It has to be recognized, though, that even at millimolar substrate concentations, the presence of the Na^+-ATPase cycle (the right-hand cycle in Fig. 9) cannot be ignored under all cation conditions.

In Appendix B a kinetic analysis of the bicyclic model is performed. Due to the lack of knowledge of the intrinsic rate constants, connecting the different enzyme conformations in Fig. 9, the argument cannot be made completely quantitative, but the considerations presented in Appendix B suggest:

(1) At micromolar substrate concentrations the

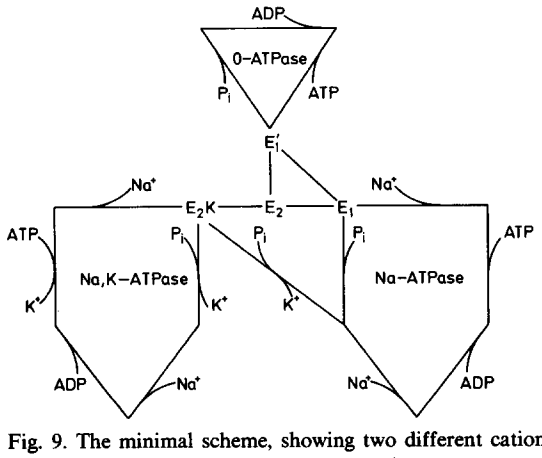

Fig. 9. The minimal scheme, showing two different cation-dependent cycles and depicting the series of events necessary to account for the results discussed in the text. The details of the enzyme intermediates have been omitted for clarity.

experimentally obtained kinetic properties for all cation conditions are those of Na^+-ATPase or K^+-inhibited Na^+-ATPase, i.e. the right-hand cycles in Fig. 9. This feature is mainly a consequence of the much larger affinity for ATP of the E_1-form than of the E_2-form so that the Na^+,K^+-cycle is not activated.

(2) At millimolar substrate concentrations the situation is more complex: (a) At $[K^+] < 5$ mM and $[Na^+] \leq 50$ mM the data are not linear in double-reciprocal plots at finite substrate concentrations.

(b) At $[K^+] \geq 5$ mM and $[Na^+] \leq 50$ mM the data appear linear, and while the slopes obtained are compatible with the slope function R_3 derived for the Na^+,K^+-cycle kinetics, the intercepts are more complicated, approaching, as $[Na^+]$ is decreased, values characteristic of Na^+-ATPase (with K^+ inhibition) which are considerably larger. This prediction is confirmed by Fig. 6. When $[Na^+] > 50$ mM the Na^+,K^+-cycle dominates, and the intercepts obtained are well represented by the function derived for the Na^+,K^+-form. This holds for the slope also.

(c) At $[K^+] < 5$ mM and $[Na^+] > 50$ mM the intercepts are compatible with the corresponding function for the Na^+,K^+-enzyme cycle, but the slope decreases rapidly as $[K^+]$ is decreased, approaching values characteristic of the Na^+-ATPase. This property is confirmed by Fig. 3.

In a recent communication Fortes and Lee [18] concluded, on the basis of estimates of the steady-state levels of phosphoenzyme intermediates using oligomycin and anthroylouabain, that the bicyclic scheme proposed here is inconsistent with their results which in their view supported the Albers-Post scheme. They propose that the slow kinetics of the phosphoenzyme intermediates observed by Nørby et al. [4], insufficient for participation in the much more rapid $(Na^+ + K^+)$-ATPase, might be explained by the presence of tightly bound ATP and/or the presence of vesicles. None of the latter suggestions are likely to hold in the dephosphorylation experiments, however, as has been shown recently by Nørby [19]. It is worth noting that for the conclusions of Fortes and Lee to hold, it is necessary to assume that E_2P (the classical K^+-sensitive phosphoenzyme) is essentially the only species to which ouabain binds, and E_1P (the classical ADP-sensitive phosphoenzyme) the only species capable of binding oligomycin. Without these a priori assumptions, their results seem compatible with the possibility that the observed decrease in the apparent rate constant for ouabain binding in the presence of K^+ is due to binding to a different species, e.g. Ex in Fig. 7, the (presumed) phosphorylated intermediate in the $(Na^+ + K^+)$-ATPase cycle (left-hand cycle in Fig. 9). A lower rate constant for ouabain binding to the K^+-sensitive enzyme than to the insensitive form, even in the absence of K^+, has been reported by Swann [20].

It should be emphasized that although the steady-state kinetic data presented here can be explained by assuming only a single (presumably phosphorylated) intermediate (denoted Ex), this does not exclude that several different (isomeric) intermediates are in fact present at steady state, in analogy to the situation for the Na^+-ATPase cycle. Steady-state data of the type considered here cannot distinguish whether or not that is the case. Thus, the species collectively denoted Ex may consist, for example, of species $E \sim P$, E-P, and $E \cdot P$, connected by reversible reaction steps (but not necessarily in rapid equilibrium with each other). A survey of the literature shows that the properties considered known of the phoshoenzyme have all been inferred from experiments in which the enzyme has been phosphorylated in the presence of Na^+ alone. Under these conditions, 25 μM MgATP is sufficient to obtain almost all the enzyme in phosphorylated form, but the phosphoenzyme so obtained is kinetically incompetent in relation to $(Na^+ + K^+)$-ATPase activity [4]. We have previously calculated [6], that at $[K^+] = 20$ mM and $[Na^+] = 150$ mM according to our model about 68% of the enzyme is present as Ex at steady state and at saturating substrate concentration. We are not aware of any measurements of the phosphoenzyme level where the phoshorylation is carried out under these conditions. Thus nothing can be said about the acid stability of any of the species making up the kinetic state Ex in Fig. 7. In that model Ex merely denotes a, presumably phosphorylated, kinetic intermediate (or set of isomeric intermediates) with kinetic properties compatible with the activity of $(Na^+ + K^+)$-ATPase.

From Fig. 7 and the values in Table II it is seen

that high-affinity ($K_d \approx 9$ mM) Na^+ binding, usually associated with the inside aspect of the Na^+-pump in whole cells, takes place to enzyme to which K^+ is already bound, probably the occluded K^+ form. Conversely, release of Na^+ from low-affinity sites ($K_d \approx 430$ mM), associated with the outside aspects of the pump, takes place prior to binding of K^+ to high-affinity sites ($K_d \approx 1.4$ mM). To the extent that the properties of the ATPase model developed here reflect the properties of the transport system in whole cells, our results thus support a transport scheme in which Na^+ and K^+ are present on the enzyme simultaneously on inside sites, but with consecutive release of Na^+ and uptake of K^+ on the outside sites. It has been shown by Sachs [21] that such a scheme ('inside simultaneous - outside consecutive'), in addition to a purely consecutive transport scheme, is quantitatively compatible with results on Na^+- and K^+-fluxes in human red cells. The consecutive nature of the outside aspect of the pump system has been demonstrated in cell ghosts by Eisner and Richards [22–24] and in squid axons by Beaugé and Di Polo [25–27].

The involvement of multiple binding sites for Na^+ and K^+ in broken membrane preparations of $(Na^+ + K^+)$-ATPase, inferred here from the kinetic data and expressed in Fig. 7, has been an established fact for a number of years [28–30]. The same features have been found in the many reports on direct cation binding (see Ref. 31 and references cited therein). Although some disagreement exists as to the precise number of sites [31], the most generally accepted figures are three sites for Na^+ and two for K^+. These figures are reflected also in the stoichiometry involved in Na^+-K^+ exchange: Na : K : ATP = 3 : 2 : 1 [32,33]. The model in Fig. 7 predicts a stoichiometry for the ATPase reaction that varies with the cationic concentrations. Some experimental support for this property is found in the work of Mullins and Brinley [34] and Brinley and Mullins [35], who in giant axons observed that the ATP-dependent cation fluxes through the membrane varied with the internal Na^+ concentration, and more recently from the work of Blostein [36,37] who showed that in inside-out red cell vesicles, the Na/ATP stoichiometry decreased when the cytoplasmic Na^+ concentration decreased. Also, there is evidence that binding of a single potassium ion suffices for the system in red blood cells to exhibit K^+-transport [38,39], and that, for external Na^+ inhibition of Na^+-K^+ exchange, binding of only a single sodium ion is required [40].

In closing we note an interesting property, conferred to the scheme in Fig. 9 by the presence of (at least) two distinct hydrolysis pathways, that of 'memory': at any time the enzyme 'remembers' which cycle it is presently engaged in because its state uniquely associates it with a particular cycle in the mechanism. Such a property is often called for in transport work but is not possessed by the Albers-Post mechanism.

Appendix A

It was shown (see previous article, Appendix) that for a simple one-substrate kinetic mechanism the slope of a double-reciprocal plot of the data depends only on the rate constants characterizing the two kinetic intermediates connected by the binding and release of substrate. When monovalent cations interfere with the mechanism, each of these kinetic states is a 'pool' of intermediates in rapid equilibrium. The mechanism may thus be written

$$\text{pool 1} \underset{k'_{-1}}{\overset{k'_1}{\rightleftharpoons}} \text{pool 2} \xrightarrow{k'_2} \tag{A1}$$

where it is understood that substrate (MgATP) binds in the step characterized by the second-order rate constant k'_1. The slope is then

$$\text{slope} = \frac{k'_{-1} + k'_2}{k'_1 k'_2 E_0} \tag{A2}$$

where E_0 is the total enzyme concentration. The apparent rate constants k'_i, and thus the slope, may be obtained as functions of the intrinsic rate constants k_i and the concentrations of ligands (Na^+ and K^+) using the method of Cha [10].

We list below a number of possible models, i.e. structure of pools, and the corresponding slopes, from the functional form of which the model compatible with the experimental data (Table I and Figs. 1 and 2) may be inferred. In the equa-

tions below the following definitions are used

$$x \equiv \frac{[Na^+]}{K_{Na}};\ y_i \equiv \frac{[K^+]}{K_{K_i}} \qquad (A3)$$

where the index i ($=1$ or 2) refers to pool number, and K_K and K_{Na} are equilibrium (dissociation) constants characterizing the ion binding. For the purpose at hand (to investigate qualitatively the type of Na^+ dependence of the K^+ inhibition of the slope) it is sufficient to consider only one sodium ion binding in all cases. For the same reason, in Table AI only the behavior as a function of x (i.e. of $[Na^+]$, Eqn. A3) of the coefficients a, b, and c in

$$\text{slope} = a + b\cdot[K^+] + c\cdot[K^+]^2 \qquad (A4)$$

is indicated. The asterisk on E indicates bound substrate.

Model (i)

$$Pool\ 1 = EK_2$$
$$Pool\ 2 = E^*K_2 - E^*K - E^* - E^*Na$$
$$k_1' = k_1;\ k_{-1}' = \frac{k_{-1}y_2^2}{(1+y_2)^2 + x};\ k_2' = \frac{k_2 x}{(1+y_2)^2 + x}$$

Model (ii)

$$Pool\ 1 = EK_2$$
$$Pool\ 2 = E^*K_2 - E^*K_2Na - E^*KNa - E^*Na$$
$$k_1' = k_1;\ k_{-1}' = \frac{k_{-1}y_2^2}{x(1+y_2)^2 + y_2};\ k_2' = \frac{k_2 x}{x(1+y_2)^2 + y_2}$$

Model (iii)

$$Pool\ 1 = EK_2 - EK_2Na$$
$$Pool\ 2 = E^*K_2Na - E^*KNa - E^*Na$$
$$k_1' = k_1\frac{x}{1+x};\ k_{-1}' = \frac{k_{-1}y_2^2}{(1+y_2)^2};\ k_2' = \frac{k_2}{(1+y_2)^2}$$

Model (iv)

$$Pool\ 1 = EK_2 - EK_2Na - EKNa - ENa$$
$$Pool\ 2 = E^*Na$$
$$k_1' = \frac{k_1 x}{x(1+y_1)^2 + y_1^2};\ k_{-1} = k_{-1};\ k_2' = k_2$$

Model (v)

$$Pool\ 1 = EK_2 - EK - E - ENa$$
$$Pool\ 2 = E^*Na$$
$$k_1' = \frac{k_1 x}{(1+y_1)^2 + x};\ k_{-1}' = k_{-1};\ k_2' = k_2$$

Model (vi)

$$Pool\ 1 = EK_2 - EK - E$$
$$Pool\ 2 = E^* - E^*Na$$
$$k_1' = \frac{k_1}{(1+y_1)^2};\ k_{-1}' = \frac{k_{-1}}{1+x};\ k_2' = \frac{k_2 x}{1+x}$$

Model (vii)

$$Pool\ 1 = EK_2 - EK - EKNa$$
$$Pool\ 2 = E^*KNa - E^*Na$$
$$k_1' = \frac{k_1 x}{1+x+y_1};\ k_{-1}' = \frac{k_{-1}y_2}{1+y_2};\ k_2' = \frac{k_2}{1+y_2}$$

Model (viii)

$$Pool\ 1 = EK_2 - EK$$
$$Pool\ 2 = E^*K - E^* - E^*Na$$
$$k_1' = \frac{k_1}{1+y_1};\ k_{-1}' = \frac{k_{-1}y_2}{1+x+y_2};\ k_2' = \frac{k_2 x}{1+x+y_2}$$

TABLE AI

BEHAVIOR FOR THE MODELS (i)–(viii) OF THE COEFFICIENTS a, b, AND c IN SLOPE $= a + b\cdot[K^+] + c\cdot[K^+]^2$ AS A FUNCTION OF $x(\equiv Na/K_{Na})$

Model	a	b	c
(i)	const	0	$1/x$
(ii)	const	0	$1/x$
(iii)	$1+1/x$	0	$1+1/x$
(iv)	const	const	$1+1/x$
(v)	$1+1/x$	$1/x$	$1/x$
(vi) [a]	$\alpha+\beta/x$	$\alpha+\beta/x$	$\alpha+\beta/x$
(vii)	$1+1/x$	$1+\text{const}/x$	$1/x$
(viii)	const	$\text{const}+1/x$	$1/x$

[a] α and β are constants, composed of intrinsic rate constants.

Appendix B

We present here some formal kinetic properties of the bicyclic model used in the main text. Since not all the kinetic parameters of the complete model are known, and a complete quantitative argument is thus precluded, we omit certain details of the complete model in Fig. 7 to simplify the equations. This does not detract from the generality of the arguments. We therefore (1) consider the action of only a single potassium ion, (2) omit the '0-ATPase' cycle, assuming that E_1 converts directly to E_2 (as is customarily done), (3) omit the low-affinity Na^+ inhibition of E_1, found previously [1], and (4) group together the several phosphorylated enzyme forms known to exist for Na^+-ATPase into a single phosphoenzyme pool.

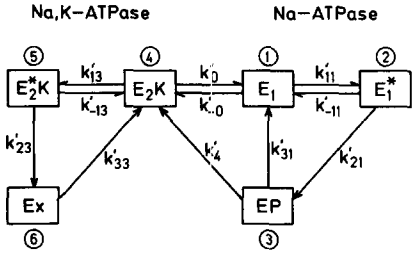

Fig. 10. The bicyclic model with omission of the '0-ATPase' cycle. Each kinetic state (box) signifies a pool of intermediates in rapid equilibrium with Na^+ and/or K^+, as appropriate. The contents of the $(Na^+ + K^+)$-ATPase pools are those shown in detail in Fig. 7, and of the Na^+-ATPase pools as described in the preceding paper [1] (omitting the weak Na^+ inhibitory site in state E_1, see text). The numbers in circles number the pools for reference in the text. The apparent (cation-dependent) rate constants are indicated.

With these simplifications, the model, derived from the scheme in Fig. 9 incorporating the results pertaining to the interaction of Na^+ and ATP with the enzyme obtained in this and in the previous paper, is shown in Fig. 10.

In this model as shown, an asterisk indicates the presence of substrate. The (primed) rate constants indicated are the effective constants, depending on the concentrations of cations, as discussed below. The numbers in circles number the pools for reference.

Using, for example, the systematic approach described by Huang [41], the steady-state initial rate equation may be derived. After a little manipulation it may be written in the following form:

$$\frac{1}{v} = \frac{R'_1R'_3(1+K'_{eq})\cdot\frac{1}{s} + R'_3Z'_1 + R'_1Z'_3(K'_{eq}+\alpha's)}{R'_3 + R'_1(K'_{eq}+\alpha's)} \tag{B1}$$

where s is the substrate concentration, and the following definitions have been used:

$$\alpha' = \frac{k'_4k'_{11}}{k'_0(k'_{31}+k'_4)}\cdot\frac{k'_{21}}{(k'_{-11}+k'_{21})} \tag{B2}$$

$$R'_1 = \frac{k'_{-11}+k'_{21}}{E_ok'_{11}k'_{21}} \tag{B3}$$

$$R'_3 = \frac{k'_{-13}+k'_{23}}{E_0k'_{13}k'_{23}} \tag{B4}$$

are the 'intrinsic slopes', and

$$Z'_1 = \frac{k'_{21}+(k'_{31}+k'_4)}{E_0k'_{21}(k'_{31}+k'_4)} \tag{B5}$$

$$Z'_3 = \frac{k'_{23}+k'_{33}}{E_0k'_{23}k'_{33}} \tag{B6}$$

are the 'intrinsic intercepts' of the two forms, i.e. the slopes and intercepts in double reciprocal plots if the two forms are studied separately. In addition, the interconversion equilibrium constant is

$$K'_{eq} = \frac{k'_{-0}}{k'_0} \tag{B7}$$

To obtain the rate equation showing explicitly the dependence on $[Na^+]$ and $[K^+]$, expressions for

the effective rate constants in terms of intrinsic (unprimed) rate constants must be inserted in Eqn. B1. For the purpose of the arguments below only some of these expressions are needed. Defining the quantities

$$x_i \equiv \frac{[Na^+]}{K_{Na_i}} \text{ and } y_i \equiv \frac{[K^+]}{K_{K_i}} \tag{B8}$$

where K_{Na_i} and K_{K_i} are the intrinsic dissociation constants for Na^+ and K^+, respectively, in pool i, the necessary equations are:

$$k'_{11} = k_{11}\frac{x_1^2(3+x_1)}{(1+x_1)^3} \tag{B9}$$

$$k'_{31} = k_{31}\frac{(1+x_3)^3}{(1+x_3)^3+y_3} \tag{B10}$$

$$k'_4 = k_4\frac{y_3}{(1+x_3)^3+y_3} \tag{B11}$$

$$k'_{-0} = k_{-0}\frac{1}{(1+x_1)^3} \tag{B12}$$

$$k'_0 = k_0\frac{1}{1+y_4(1+x_4)^3}. \tag{B13}$$

Also needed is a property of R'_3, Eqn. B3:

$$R'_3 = \frac{k_{-13}\cdot y_5 + k_{23}}{E_0 k_{13} k_{23}\cdot y_4}\cdot\frac{1+y_4(1+x_4)^3}{(1+x_4)^3-1} \tag{B14}$$

$$R'_3 \to \infty \text{ as } K^+ \to 0 \text{ (i.e. } y_4,\ y_5 \to 0) \tag{B15}$$

Using Eqns. B8–B12, Eqn. B1 may now be written

$$\frac{1}{v} = \frac{R'_1R'_3(1+C_1K_{eq})\cdot\frac{1}{s}}{R'_3+R'_1[C_1K_{eq}+C_2\cdot\alpha s]} + \frac{R'_3Z'_1+R'_1Z'_3[C_1K_{eq}+C_2\cdot\alpha s]}{R'_3+R'_1[C_1K_{eq}+C_2\cdot\alpha s]} \tag{B16}$$

where the coefficients C_1 and C_2 are:

$$C_1 = \frac{1+y_4(1+x_4)^3}{(1+x_1)^3} \tag{B17}$$

$$C_2 = \frac{y_3x_1^2(3+x_1)[1+y_4(1+x_4)^3]}{(1+x_1)^3[(1+x_3)^3+y_3]} \tag{B18}$$

and

$$K_{eq} = \frac{k_{-0}}{k_0};\ \alpha = \frac{k_4k_{11}}{k_0(k_{31}+k_4)}\cdot\frac{k_{21}}{(k_{-11}+k_{21})} \tag{B19}$$

When $[K^+] = 0$, the cycle 4-5-6-4 and the transition $3 \to 4$ in Fig. 10 are inoperative. This corresponds to Na^+-ATPase conditions. Formally, the appropriate rate equation may be derived from Eqn. B16 by finding the limit as $R'_3 \to \infty$:

$$\frac{1}{v} = R'_1\left(1+\frac{K_{eq}}{(1+x_1)^3}\right)\cdot\frac{1}{s} + Z'_1 \tag{B20}$$

and Eqn. B17, with $y_4 = 0$, has been used. This equation, with appropriate changes due to the presence of the '0-ATPase' cycle, was studied in the preceding paper. On the other hand, at finite K^+ and very large substrate concentration ($s \to \infty$) the activity obtained from Eqn. B16

$$\frac{1}{v} \approx Z'_3 \tag{B21}$$

At intermediate substrate concentrations and in the presence of Na^+ and K^+, Eqn. B16 shows that the model under consideration never exhibits Michaelis-Menten behavior in a strict sense.

We have previously [42] pointed out that when, at constant Na^+ and K^+ concentrations, the substrate concentration is increased from micromolar to millimolar values, the steady-state nonlinear substrate curve obtained reflects a gradual transition from 'all enzyme in the Na^+-ATPase cycle' (i.e., the cycle 1-2-3-1 in Fig. 10) to 'all enzyme in the $(Na^+ + K^+)$-ATPase cycle' (i.e. cycle 4-5-6-4). It may be, however, that within a limited range of substrate concentrations, the experimental uncertainty may mask the nonlinearity of the data. This would be true when the activity of the Na^+-ATPase cycle is a small fraction of that in the other cycle. The question is, then, what are the slopes and intercepts of such data in relation to the 'intrinsic' values? We note from Eqn. B16 that when the second term in square brackets is not dominating, as would be the case for small s and C_2, the rate expression may be considered approximately linear in $1/s$:

$$\frac{1}{v} = R^*\cdot\frac{1}{s} + Z^* \tag{B22}$$

with 'slope' R^* and 'intercept' Z^*

$$R^* = \frac{R'_1 R'_3 (1 + C_1 \cdot K_{eq})}{R'_3 + R'_1 [C_1 K_{eq} + C_2 \cdot \alpha s]} \quad \text{(B23)}$$

$$Z^* = \frac{R'_3 Z'_1 + R'_1 Z'_3 [C_1 K_{eq} + C_2 \cdot \alpha s]}{R'_3 + R'_1 [C_1 K_{eq} + C_2 \cdot \alpha s]} \quad \text{(B24)}$$

We have no knowledge of the rate constants k_4, k_0, and k_{31}, nor of the equilibrium constant K_{eq}, so only a semiquantitative argument can be given. We first note that from the kinetic data evaluated in this and the preceding paper, typical values at equal cation concentrations, of R'_1, R'_3, Z'_1, and Z'_3 are such that

$$R'_3 \approx 30\ R'_1 \quad \text{(B25)}$$

$$Z'_1 \approx 25\ Z'_3. \quad \text{(B26)}$$

From Eqns. B23 and B24 it is seen that if the 'R'_3-terms' dominate, we have $R^* \approx R'_1(1 + C_1 K_{eq})$ and $Z^* \approx Z'_1$, as for Na^+-ATPase, while if the 'R'_1-terms' are dominating, $R^* \approx R'_3$ and $Z^* \approx Z'_3$. In either case the appropriate function can be analyzed with the data. The point to be emphasized here is that with a certain, limited range of substrate concentrations, e.g. $s \approx 1$ mM, the relative importance of the terms just discussed will change when the cation concentrations change, due to the dependence of C_1 and C_2 on $[Na^+]$ and $[K^+]$, and that, when the terms are of equal importance, the slopes and intercepts obtained from the data, R^* and Z^*, are complicated functions of the 'intrinsic slopes and intercepts', R'_1, R'_3, Z'_1, and Z'_3. If these latter are known as functions of the cation concentrations from data obtained under appropriate circumstances (this we believe to be the case here), the model in Fig. 10 thus predicts that the intercepts and/or slopes obtained under the conditions just described, should not be expected to fit either 'intrinsic' function (R or Z).

The lack of knowledge of K_{eq} and of the term multiplying C_2 in Eqn. B16 precludes a quantitative argument. But since these terms, for a given, limited, substrate range are (almost) constant, we can illustrate the above arguments by an order of magnitude calculation. For this purpose the following values, based on the work reported here and on earlier work [6], for the pool dissociation constants were used:

$$K_{K3} \approx 3 \text{ mM} ; \ K_{K4} \approx 1 \text{ mM}$$

$$K_{Na1} \approx 5 \text{ mM} ; \ K_{Na3} \approx 400 \text{ mM} ; \ K_{Na4} \approx 10 \text{ mM} \quad \text{(B27)}$$

For $[K^+] = 30$ mM we obtain:

$$\text{at } [Na^+] = 5 \text{ mM}: \ C_1 = 12.8 ; \ C_2 = 46.3 \quad \text{(B28)}$$

$$\text{at } [Na^+] = 150 \text{ mM}: \ C_1 = 4.1 ; \ C_2 = 2.4 \cdot 10^4 \quad \text{(B29)}$$

These values, in conjunction with Eqns. B25 and B26 suggest that at $[Na^+] = 150$ mM $R^* \approx R'_3$ and $Z^* \approx Z'_3$ (Eqns. B23 and B24), while this may not be the case at $[Na^+] = 5$ mM, if K_{eq} and the term multiplying C_2 are not excessive.

Another feature predicted from the model is the following: If $[K^+]$ becomes very small at high Na^+ concentrations, C_2 (Eqn. B18) is decreased, and R'_3 increases (Eqn. B15). Hence, at these small K^+ concentrations the observed slope R^* (Eqn. B23) approaches the value $R'_1(1 + C_1 K_{eq})$ characteristic of Na^+-ATPase even at substrate concentrations in the millimolar range. Thus, because of the relation B25, a considerable decrease of the observed slope is expected as the K^+ concentration is decreased to low values (a few millimolar and below). This is the observed behavior.

Acknowledgements

We are grateful to Mrs. Vinni Ravn for her painstaking care with the experimental work. Financial support through grants (to L.P.) from the Danish Medical Research Council, the P. Carl Pedersen Foundation, and from Ingeborg and Leo Dannin's Foundation for Scientific Research is gratefully acknowledged.

References

1 Plesner, L. and Plesner, I.W. (1985) Biochim. Biophys. Acta 818, 222–234
2 Plesner, L. and Plesner, I.W. (1981) Biochim. Biophys. Acta 643, 449–462
3 Plesner, L. and Plesner, I.W. (1985) in The Sodium Pump-Fourth International Conference on Na,K-ATPase (Glynn, I.M. and Ellory, C.J., eds.), pp. 469–474, The Company of Biologists, Cambridge
4 Nørby, J.G., Klodos, I. and Christiansen, N.O. (1983) J. Gen. Physiol. 82, 725-759

5 Plesner, I.W., Plesner, L., Nørby, J.G. and Klodos, I. (1981) Biochim. Biophys. Acta 643, 483–494
6 Plesner, I.W. and Plesner, L. (1981) Biochim. Biophys. Acta 648, 231–246
7 Ottolenghi, P. (1975) Biochem. J. 151, 61–66
8 Lindberg, O. and Ernster, L. (1956) in Methods of Biochemical Analysis (Gliek, G., ed.), Vol. 3, pp. 1–22, Interscience, New York
9 Yamaguchi, M. and Tonomura, Y. (1979) J. Biochem. (Tokyo) 86, 509–523
10 Cha, S. (1968) J. Biol. Chem. 243, 820–825
11 Jørgensen, P.L. and Petersen, J. (1982) Biochim. Biophys. Acta 705, 38–47
12 Jensen, J. and Ottolenghi, P. (1983) in Current Topics in Membranes and Transport (Hoffman, J.F. and Forbush, B., III, eds.), Vol. 19, pp. 223–227, Academic Press, New York
13 Glynn, I.M. and Richards, D.E. (1982) J. Physiol. (London) 330, 17–43
14 Glynn, I.M., Richards, D.E. and Hara, Y. (1985) in The Sodium Pump-Fourth International Conference on Na,K-ATPase (Glynn, I.M. and Ellory, C.J., eds.), pp. 589–598, The Company of Biologists, Cambridge
15 Forbush, B., III (1985) in The Sodium Pump-Fourth International Conference on Na,K-ATPase (Glynn, I.M. and Ellory, C.J., eds.), pp. 599–611, The Company of Biologists, Cambridge
16 Skou, J.C. and Esmann, M. (1980) Biochim. Biophys. Acta 601, 386–402
17 Plesner, I.W. and Plesner, L. (1985) in The Sodium Pump-Fourth International Conference on Na,K-ATPase (Glynn, I.M. and Ellory, C.J., eds.), pp. 457–467, The Company of Biologists, Cambridge
18 Fortes, P.A.G. and Lee, J.A. (1984) J. Biol. Chem. 259, 11176–11179
19 Nørby, J.G. (1985) in The Sodium Pump-Fourth International Conference on Na,K-ATPase (Glynn, I.M. and Ellory, C.J., eds.), pp. 399–407, The Company of Biologists, Cambridge
20 Swann, A.C. (1985) in The Sodium Pump-Fourth Internatinal Conference on Na,K-ATPase (Glynn, I.M. and Ellory, C.J., eds.), pp. 273–275, The Company of Biologists, Cambridge
21 Sachs, J.R. (1980) J. Physiol. 302, 219–240
22 Eisner, D.A. and Richards, D.E. (1981) J. Physiol. 319, 403–418
23 Eisner, D.A. and Richards, D.E. (1982) J. Physiol. 326, 1–10
24 Eisner, D.A. and Richards, D.E. (1983) in Current Topics in Membranes and Transport (Hoffman, J.F. and Forbush, B., III, eds.), Vol. 19, pp. 547–551, Academic Press, New York
25 Beaugé, L.A. and Di Polo, R. (1979) Biochim. Biophys. Acta 553, 495–500
26 Beaugé, L.A. and Di Polo, R. (1981) J. Physiol. 314, 457–480
27 Beaugé, L.A. and Di Polo, R. (1983) in Current Topics in Membranes and Transport (Hoffman, J.F. and Forbush, B., III, eds.), Vol. 19, pp. 643–647, Academic Press, New York
28 Skou, J.C. (1965) Physiol. Rev. 45, 596–617
29 Lindenmayer, G.E., Schwartz, A. and Thompson, H.K. (1974) J. Physiol. (London) 236, 1–28
30 Robinson, J.D. (1970) Arch. Biochem. Biophys. 139, 17–27
31 Jensen, J., Nørby, J.G. and Ottolenghi, P. (1984) J. Physiol. 346, 219–241
32 Garrahan, P.J. and Glynn, I.M. (1967) J. Physiol. (London) 192, 217–235
33 Sen, A.K. and Post, R.L. (1964) J. Biol. Chem. 239, 345–352
34 Mullins, L.J. and Brinley, F.J. (1969) J. Gen. Physiol. 53, 704–740
35 Brinley, F.J. and Mullins, L.J. (1974) Ann. N.Y. Acad. Sci. 242, 406–432
36 Blostein, R. (1983) J. Biol. Chem. 258, 12228–12232
37 Blostein, R. (1985) J. Biol. Chem. 260, 829–833
38 Kropp, D.L. and Sachs, J.R. (1977) J. Physiol. 264, 471–487
39 Sachs, J.R. (1977) J. Physiol. 264, 449–470
40 Sachs, J.R. (1967) J. Clinic. Invest. 46, 1433–1441
41 Huang, C.Y. (1979) in Methods in Enzymology (Purich, D.L., ed.), Vol. 63, pp. 54–84, Academic Press, New York
42 Plesner, I.W. (1983) in Current Topics in Membranes and Transport (Hoffman, J.F. and Forbush, B., III, eds.), Vol. 19, pp. 587–590, Academic Press, New York